

## A UNIVERSAL NEUTRAL GAS PROFILE FOR NEARBY DISK GALAXIES

F. BIGIEL<sup>1</sup> AND L. BLITZ<sup>2</sup>

*Accepted for publication in the Astrophysical Journal*

### ABSTRACT

Based on sensitive CO measurements from HERACLES and H I data from THINGS, we show that the azimuthally averaged radial distribution of the neutral gas surface density ( $\Sigma_{\text{HI}} + \Sigma_{\text{H}_2}$ ) in 33 nearby spiral galaxies exhibits a well-constrained universal exponential distribution beyond  $0.2 \times r_{25}$  (inside of which the scatter is large) with less than a factor of two scatter out to two optical radii  $r_{25}$ . Scaling the radius to  $r_{25}$  and the total gas surface density to the surface density at the transition radius, i.e., where  $\Sigma_{\text{HI}}$  and  $\Sigma_{\text{H}_2}$  are equal, as well as removing galaxies that are interacting with their environment, yields a tightly constrained exponential fit with average scale length  $0.61 \pm 0.06 r_{25}$ . In this case, the scatter reduces to less than 40% across the optical disks (and remains below a factor of two at larger radii). We show that the tight exponential distribution of neutral gas implies that the total neutral gas mass of nearby disk galaxies depends primarily on the size of the *stellar* disk (influenced to some degree by the great variability of  $\Sigma_{\text{H}_2}$  inside  $0.2 \times r_{25}$ ). The derived prescription predicts the total gas mass in our sub-sample of 17 non-interacting disk galaxies to within a factor of two. Given the short timescale over which star formation depletes the H<sub>2</sub> content of these galaxies and the large range of  $r_{25}$  in our sample, there appears to be some mechanism leading to these largely self-similar radial gas distributions in nearby disk galaxies.

*Subject headings:* Galaxies:ISM — Galaxies:Evolution

### 1. INTRODUCTION

Scaling relations are important because they are often thought to be manifestations of some underlying fundamental physical processes. They also make it possible to determine properties of a system with incomplete measurements to within the scatter of the scaling. The total neutral gas content of galaxies has long defied such characterizations because of the wide diversity of previously observed gas surface density distributions (see, e.g., Helfer et al. 2003). This was at least partly due to the lack of comprehensive, resolved, extended and deep observations of atomic (H I) and molecular gas (H<sub>2</sub>) across the disks of a significant sample of galaxies. This limitation has been overcome by the availability of new radio surveys providing sensitive H I and CO (the standard tracer for H<sub>2</sub>) radio data, tracing the gas content of many nearby galaxies out to large galactocentric radii (THINGS, HERACLES, Walter et al. 2008; Leroy et al. 2009).

With these data sets in hand, we can now re-assess the azimuthally averaged gas distributions (radial profiles) in nearby spiral galaxies. Both HI and CO profiles tend to show quite distinct behavior: the HI surface density distributions are often depressed in the centers, increasing in the inner disk and slowly declining in the outer regions. Furthermore, the surface density in the outer regions can be affected by environmental factors such as interaction with companions or truncation due to the ram pressure stripping by the hot gas in galaxy clusters (Cayatte et al. 1994). As for the molecular gas, it tends to fall off much more sharply than the HI in

an approximately exponential fashion that varies from galaxy to galaxy (Young & Scoville 1982; Regan et al. 2001; Leroy et al. 2008; Bigiel et al. 2008).

We show in this paper, however, that when the totality of the neutral (i.e., atomic and molecular) gas in normal spirals is considered based on the data from these new surveys, and the profiles are properly scaled, the gas exhibits a radial profile shape that is remarkably constant from galaxy to galaxy. The gas surface density is found to vary by no more than about a factor of two from this average profile across the optical disk and even beyond. We show that the scatter reduces even further when we eliminate galaxies that are interacting with their environment.

### 2. DATA & METHODOLOGY

In this paper we use radial profiles (i.e., azimuthal averages in tilted rings) of atomic hydrogen,  $\Sigma_{\text{HI}}$ , molecular hydrogen (as traced by CO emission),  $\Sigma_{\text{H}_2}$ , and the total gas surface density  $\Sigma_{\text{gas}} = \Sigma_{\text{HI}} + \Sigma_{\text{H}_2}$ . We derive the H<sub>2</sub> profiles out to one and the H I and total gas profiles from the centers out to two optical radii  $r_{25}$ , which is defined as the 25 mag arcsec<sup>-2</sup> B-band isophote. We will refer to the regime within  $r_{25}$  as the optical disk.

The VLA THINGS survey (The HI Nearby Galaxy Survey, Walter et al. 2008), provides sensitive ( $\sigma_{\text{HI}} \approx 0.5 M_{\odot} \text{ pc}^{-2}$  at 30'' resolution), extended ( $\sim 0.5^{\circ}$  field-of-view) HI data. These data, together with new and archival data for some of the target galaxies, allow us to track the HI distribution out to  $2 \times r_{25}$  with good sensitivity.

The IRAM 30m survey HERACLES provides the distribution of <sup>12</sup>CO(2-1) emission in our sample galaxies (HERA CO Line Extragalactic Survey, Leroy et al. 2009). HERACLES provides sensitive ( $\sigma_{\text{H}_2} \approx 5 M_{\odot} \text{ pc}^{-2}$  for the most distant, face-on systems) data covering the

<sup>1</sup>Institut für theoretische Astrophysik, Zentrum für Astronomie der Universität Heidelberg, Albert-Ueberle Str. 2, 69120 Heidelberg, Germany; bigiel@uni-heidelberg.de

<sup>2</sup>Department of Astronomy, Radio Astronomy Laboratory, University of California at Berkeley, CA 94720, USA

entire optical disk out to  $r_{25}$ . The quoted  $\text{H}_2$  surface densities in this paper include a Galactic CO-to- $\text{H}_2$  conversion factor  $X_{\text{CO}} = 2 \times 10^{20} \text{ cm}^{-2} (\text{K km s}^{-1})^{-1}$  and a CO line ratio  $I_{\text{CO}(2-1)}/I_{\text{CO}(1-0)} = 0.7$  (see Leroy et al. 2012). Because H I can be observed out to much larger radii for individual lines-of-sight, Schruba et al. (2011) used the velocity information from the H I as a prior to stack individual CO spectra. This technique allows one to probe down to  $\sigma_{\text{H}_2} \approx 1 \text{ M}_\odot \text{ pc}^{-2}$  and thus to derive radial CO profiles out to the edge of the optical disk ( $\sim r_{25}$ ). This represents a significant improvement over previous studies and we adopt their radial  $\text{H}_2$  profiles derived from this approach.

We thus focus our analysis on the data and galaxy sample presented in Schruba et al. (2011), which consists of 33 nearby, star-forming disk galaxies (excluding edge-on, low-mass and low-metallicity systems). All quoted surface densities in this paper include the contribution from helium (a factor of 1.36) and are corrected for inclination. We refer the reader to Schruba et al. (2011) for further details and references regarding sample selection and properties, H I and CO datasets, the stacking technique for the CO data and the conversion of line intensities to surface densities.

We stress that it is the combination of such deep, wide-field CO data, the stacking technique as well as the sensitive HI data, which permits to derive unprecedentedly accurate radial distributions of the atomic, molecular and total gas across galaxy disks. These radial profiles are shown for each galaxy in the galaxy atlas in the Appendix of Schruba et al. (2011) (note, however, that we extend their H I profiles out to  $2 \times r_{25}$ ).

We also include radial gas profiles for the Milky Way for comparison. We adopt the H I and  $\text{H}_2$  profiles from Dame (1993)<sup>3</sup>, adjust the latter to match our adopted value for  $X_{\text{CO}}$  and include the contribution from helium. We assume  $r_{25} = 16 \text{ kpc}$ , based on the observation that H II regions, planetary nebulae and carbon stars seem to disappear at about  $2 \times R_\odot$  in the Milky Way (Fich & Blitz 1984; Schneider & Terzian 1983; Schechter et al. 1988).

### 3. RESULTS

#### 3.1. Unscaled Radial Profiles

Figure 1 shows the H I,  $\text{H}_2$  and total gas surface density profiles of the 33 sample galaxies and the Milky Way. Radially slightly less extended versions of these profiles as well as the H I and CO maps they are derived from are shown for each of our sample galaxies in Schruba et al. (2011). We refer the reader to the Appendix of that paper to match individual galaxies to particular profiles.

The top panel of Figure 1 shows the H I profiles. They are generally relatively flat and show a great deal of scatter with little apparent regularity except for a concentration just below  $\sim 10 \text{ M}_\odot \text{ pc}^{-2}$  for radii  $r \lesssim 10 - 12 \text{ kpc}$ . This is the maximum H I surface density (for near solar-metallicity galaxies) before the interstellar medium (ISM) becomes primarily molecular (Martin & Kennicutt 2001; Wong & Blitz 2002; Leroy et al. 2008; Bigiel et al. 2008). Note that the

profiles fill almost all of the “phase space” between 1 and  $10 \text{ M}_\odot \text{ pc}^{-2}$  at all radii. Some profiles are truncated and decrease steeply: these are often interacting systems or cluster members. In the inner parts, many galaxies show a more or less pronounced depression. These central “H I holes” are usually regions where the ISM is predominantly molecular (the  $\Sigma_{\text{H}_2}/\Sigma_{\text{H I}}$  ratio increases roughly exponentially with decreasing radius; e.g., Leroy et al. 2008; Bigiel et al. 2008). The Milky Way H I profile agrees well with the overall trend: H I-deficient in the center and relatively flat throughout at  $\Sigma_{\text{H I}} \approx 5 - 7 \text{ M}_\odot \text{ pc}^{-2}$ .

Almost all  $\text{H}_2$  profiles in the middle panel show an exponential-like decline. The scale length, however, is different from galaxy-to-galaxy, i.e. some profiles are steeper than others. Like the H I profiles, the  $\text{H}_2$  profiles fill almost all of the “phase space” up to the most molecule-rich galaxy. In their inner parts, many galaxies deviate from this exponential trend and the  $\text{H}_2$  surface density rises much more steeply (see also Regan et al. 2001). Even when averaged over many square kpc, some galaxies reach surface densities of many  $100 \text{ M}_\odot \text{ pc}^{-2}$  in the inner parts, quite similar to what is observed in starburst galaxies (e.g., Kennicutt 1998). The Milky Way profile also declines roughly exponentially from  $r \approx 5 \text{ kpc}$  on outward, but shows a depression at smaller radii. Where it declines exponentially, it does so with a scale length typical of many of the other galaxies.

The plot of the total gas profiles is given in the bottom panel and shows that the combination of the relatively flat H I profiles (over large parts of the radius range considered here) and the exponential  $\text{H}_2$  profiles leads to somewhat more coherent total gas profiles for many of the galaxies than do either the H I or  $\text{H}_2$  profiles alone. The total gas profiles cluster at surface densities between a few and a few times  $10 \text{ M}_\odot \text{ pc}^{-2}$  between  $r \approx 2 - 12 \text{ kpc}$ . The Milky Way profile falls quite in the middle of the bulk of the profiles and thus its averaged gas distribution matches that of most of the other galaxies well.

We also show mean data values (red points) and associated  $1\sigma$  RMS scatter of the profiles in 2 kpc wide bins (note that the means are plotted in the middle of these bins). We exclude the central 2 kpc for the binning where the profiles rise much more steeply than further out. The relative scatter ranges from  $\sim 60\%$  to  $\sim 80\%$  within the optical disks, i.e., for  $r < r_{25}$ , and remains within a factor of two even at large radii where the profiles begin to flare significantly.

The red line shows an ordinary-least-squares (OLS) fit to the means and yields an average scale length of 6.1 kpc with standard deviation 0.3 kpc. Even though the fit is relatively well constrained (reflected by the small standard deviation), we estimate the impact of several other factors on the fit result by doing the following: 1) we add noise to each data point (mean) and re-fit, 2) we bootstrap (sampling profiles from the ensemble allowing repetition), 3) we vary the radius range to fit over and 4) we vary the bin size we use to derive the means. The first method is an uncertainty estimate based on the error on the mean in each bin, the second addresses how much individual profiles drive the fit and the last two approaches probe the impact of our specific choices for radius range and bin size. Adding noise as well as varying radius

<sup>3</sup> We use their H I profile based on the Kulkarni et al. (1982, KBH) rotation curve and the  $\text{H}_2$  profile following Bigiel (1991) at large radii.

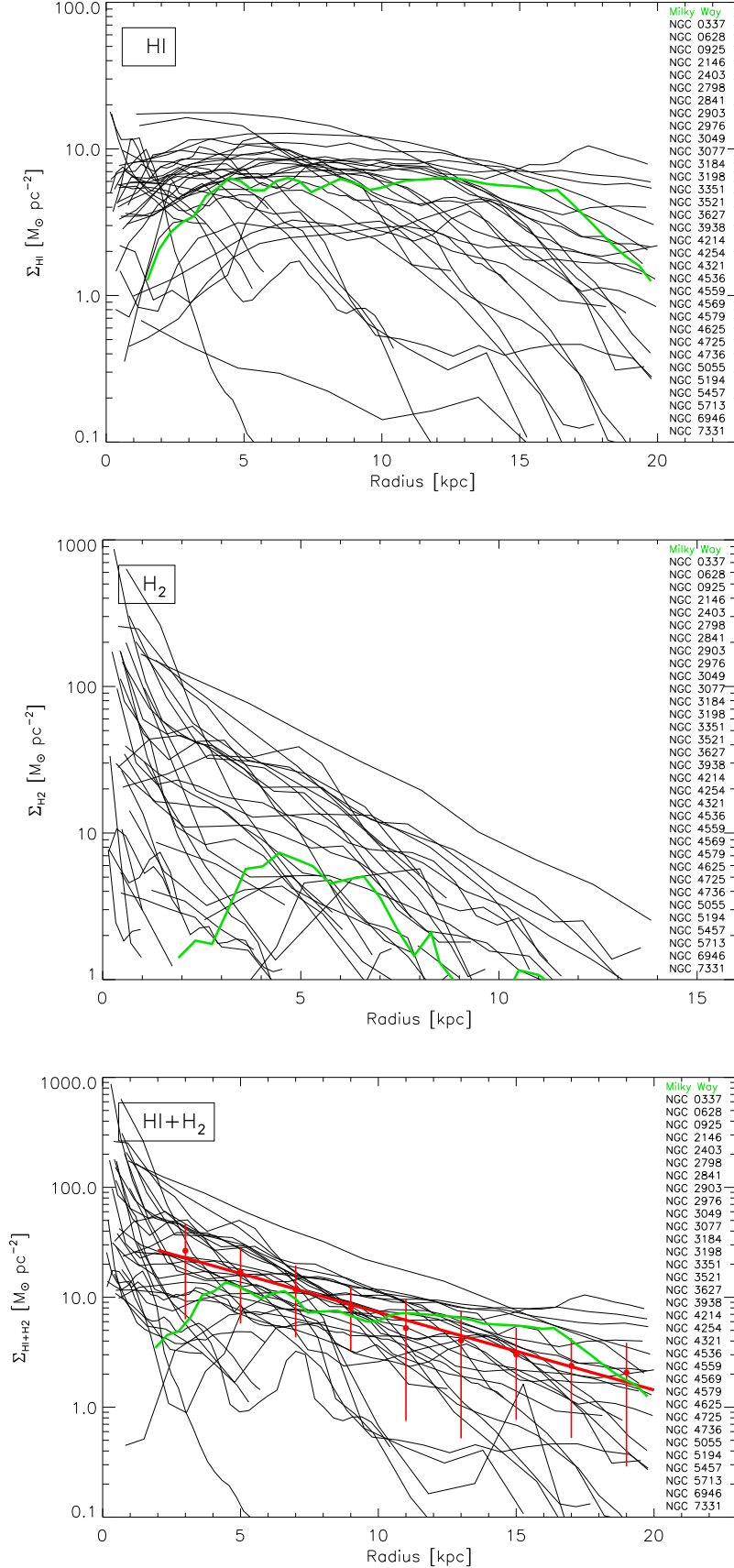


FIG. 1.— Radial profiles of the surface densities of atomic gas ( $\Sigma_{\text{HI}}$ , top panel), molecular gas ( $\Sigma_{\text{H}_2}$ , middle panel) and total gas ( $\Sigma_{\text{gas}} = \Sigma_{\text{HI}} + \Sigma_{\text{H}_2}$ , bottom panel) for 33 nearby, star-forming disk galaxies and the Milky Way. While the H I profiles are generally flat and concentrate just below  $10 M_{\odot} \text{pc}^{-2}$ , the  $\text{H}_2$  profiles decline approximately exponentially. An exponential fit to the binned means (red points; error bars show the RMS scatter) characterizes the bulk of the total gas profiles well and the scatter about the fit remains within a factor of two even at large radii.

range and bin size lead to an uncertainty  $< 0.5$  kpc. Bootstrapping leads to an uncertainty of  $\sim 0.7$  kpc, which we adopt as our uncertainty on the fit so that we quote the mean scale length of the unscaled total gas profiles as  $6.1 \pm 0.7$  kpc. We will show in the following that the agreement among these profiles can be improved further by scaling both axes the right way and by focusing on non-interacting galaxies.

### 3.2. Scaled Radial Profiles

By measuring the radius in physical units (kpc), intrinsic differences in the size of the galaxies will lead to scatter in the profile distribution. This can be accounted for if the x-axis (radius) is normalized by the optical radius ( $r_{25}$ ) of the galaxy. This scaling reduces the scatter to 40 – 60% across the optical disk (beyond which it reaches up to 100% at large radii, similar to the unscaled profiles). This is notably less than the 60 – 80% in the unscaled case above.

Blitz & Rosolowsky (2004) noted, that there is a natural scale to the gas in normal spirals if the conversion from H I to H<sub>2</sub> is governed primarily by the midplane hydrostatic pressure in galactic disks. In that case, the location where the gas in the disk goes from being primarily molecular in the inner regions, to where it becomes primarily atomic in the outer regions, should occur at a constant *stellar* surface density. They showed that for the 28 galaxies they analyzed, this constancy is good to about 40% and has a value of  $\sim 120 M_{\odot} \text{ pc}^{-2}$ . Leroy et al. (2008) reached the same conclusion (although they derived a stellar surface density of  $81 \pm 25 M_{\odot} \text{ pc}^{-2}$ ), using a combination of HERACLES, THINGS and BIMA SONG (BIMA Survey of Nearby Galaxies, Helfer et al. 2003) data for 23 nearby galaxies. We determine this transition radius (i.e., where  $\Sigma_{\text{HI}} = \Sigma_{\text{H}_2}$ ) directly for each galaxy from the radial profiles (typically the transition occurs at  $\Sigma_{\text{gas}} \approx 14 M_{\odot} \text{ pc}^{-2}$ ).

In Figure 2 we show the profiles one obtains if both scalings are applied: the radius is normalized to the size of the optical disk (x-axis) and the gas surface density is scaled to the value of  $\Sigma_{\text{gas}}$  at the transition radius (y-axis). For six galaxies the transition radius cannot be readily determined: the ISM in these galaxies is either entirely dominated by H I (NGC 337, NGC 925, NGC 4214, NGC 4559) or entirely H<sub>2</sub> dominated (NGC 4569, NGC 2798). We will not include these galaxies in this plot and the following.

The red points in Figure 2 show mean values and  $1\sigma$  scatter in  $0.2 \times r_{25}$ -wide bins. The scatter increases from  $\sim 35\%$  to  $\sim 80\%$  at large radii where the profiles begin to flare. Across the optical disks the scatter is between 35% and 50%. While the normalization of the x-axis has a bigger impact reducing the scatter, the additional scaling of the surface density reduces the scatter further to 50% or less within the optical disks and to less than a factor of two even at large radii. The minimum scatter of 35% is almost a factor of two improvement compared to the minimum scatter of 60% for the unscaled case. This matches the visual impression that the scaled profiles in Figure 2 show a remarkably tight distribution.

The red line shows the OLS fit to the means and yields an average scale length of  $0.48 \pm 0.04 r_{25}$ , where the error is the standard deviation. Following the approach de-

scribed in Section 3.1, we estimate the uncertainty of the fitted scale length in several ways. We find that bootstrapping and varying the radius range dominate the uncertainties and we quote our final fit result as  $0.48 \pm 0.06 r_{25}$ .

The gas distribution, particularly in the outer parts, can be significantly affected by interactions with other galaxies in groups or clusters or by ram pressure stripping from a hot intracluster medium. Oftentimes these interactions result in truncated H I profiles, driving the scatter in the profile ensemble.

In addition to the six galaxies with uncertain transition radii above, we further eliminate 10 galaxies that exhibit evidence for interactions with their environments. These are galaxies that show signs of strong tidal interactions in their HI distributions and those which are members of the Virgo or Coma clusters subject to ram-pressure stripping. These galaxies are: NGC 2146, NGC 2976, NGC 3077, NGC 3627, NGC 4254, NGC 4321, NGC 4579, NGC 4725, NGC 5194, NGC 5713 (note that NGC 2798 and NGC 4569 would be part of this list too, but are already excluded based on the unclear transition radius in these galaxies).

Figure 3 shows the plot that results if both axes are scaled as in Figure 2, but after removing the interacting galaxies. For the remaining 17 galaxies, the scatter within the optical disks reduces to 25 – 40% and remains between  $\sim 80$  – 90% beyond  $r_{25}$ . The Milky Way profile is a good match to the overall trend. The ensemble constitutes a tight, well-defined exponential distribution across the optical disk with deviations in the centers and flaring in the outer disks. The fit yields a scale length of  $0.61 \pm 0.03 r_{25}$  and we quote our final result based on bootstrapping as the dominant source of uncertainty as  $0.61 \pm 0.06 r_{25}$ .

## 4. DISCUSSION

Figure 3 shows that galaxies not interacting with their environment exhibit a tight exponential distribution of their total gas content when the radius is scaled to the optical radius and the surface density of the gas is scaled to the surface density of the gas at the transition radius. The scaling relation for disk galaxies we derive is:

$$\frac{\Sigma_{\text{gas}}}{\Sigma_{\text{trans}}} = 2.1 \times e^{-1.65 \times r/r_{25}}, \quad (1)$$

where  $\Sigma_{\text{trans}}$  is the surface density of the gas at the transition radius. The factors 2.1 and  $-1.65$  are obtained from the y-intercept and slope of the exponential fit in Figure 3. This implies that for these disk galaxies the total mass of neutral gas,  $M_{\text{gas}}$ , is given by

$$M_{\text{gas}} = 2\pi \times 2.1 \times \Sigma_{\text{trans}} \times r_{25}^2 \times X, \quad (2)$$

where the factor X depends on how far out from the center one integrates Equation 1. Integrating out to the optical radius  $r_{25}$  yields  $X = 0.18$ , out to  $2 \times r_{25}$  yields  $X = 0.31$  and integrating to infinity yields  $X = 0.37$ .

Equation 2 shows that for any given maximum radius,  $M_{\text{gas}}$  depends only on  $r_{25}^2$  and  $\Sigma_{\text{trans}}$ .  $\Sigma_{\text{trans}}$  does not vary a great deal from galaxy to galaxy and has a typical value of about  $14 M_{\odot} \text{ pc}^{-2}$  (also compare Leroy et al. 2008; Bigiel et al. 2008). Thus,  $M_{\text{gas}}$  depends primarily

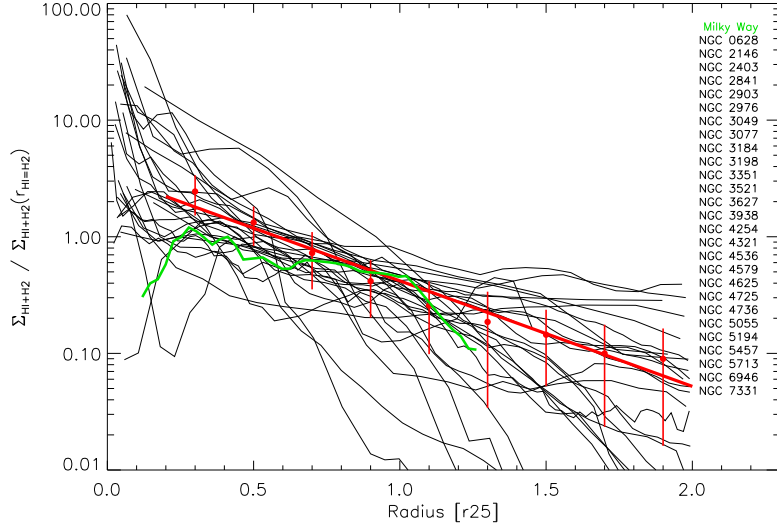


FIG. 2.— Scaled radial profiles for the galaxy ensemble: the radius (x-axis) is normalized to the size of the optical disk and  $\Sigma_{\text{gas}}$  (y-axis) is scaled to the value at the transition radius, i.e., where the ISM transitions from being primarily molecular to being primarily atomic. The combined distribution of profiles is remarkably tight, including the Milky Way profile which is right in the middle of the galaxy ensemble. The exponential fit to the means is well constrained and the scatter is reduced significantly compared to the unscaled profiles in the bottom panel of Figure 1.

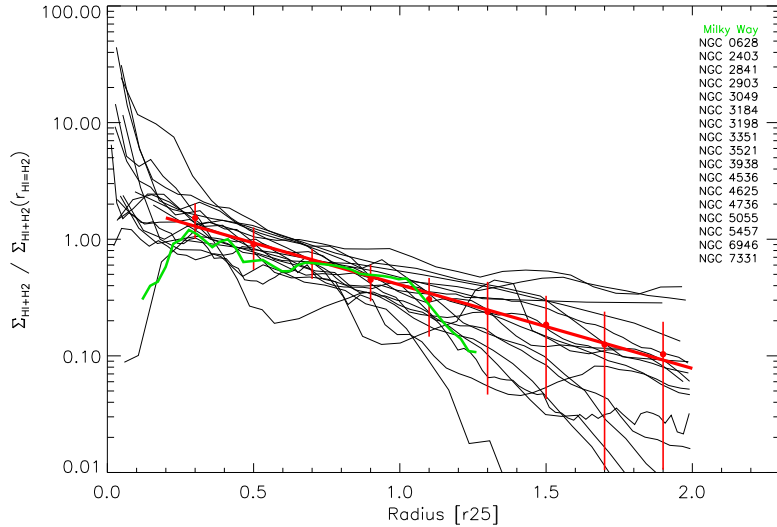


FIG. 3.— Scaled radial profiles as in Figure 2, but after removing galaxies showing signs of interaction with their environment. The distribution of these disk galaxy profiles is extremely tight, with a scatter across the optical disk of only 25 – 40% and a scale length of the exponential fit of  $\sim 0.61 r_{25}$ . The Milky Way profile is an excellent match to the average trend.

on  $r_{25}^2$ , which varies by two orders of magnitude for the galaxies plotted.

This leads to the surprising result that the mass of neutral hydrogen gas depends mostly on the size of the stellar disk and that the gas arranges itself somehow into a distribution that is self-similar among galaxies. The result also implies that except for the region of a galaxy at  $\lesssim 0.2 r_{25}$ , which is highly variable, the total neutral gas mass of a disk galaxy at  $z = 0$  can be estimated if  $r_{25}$ , i.e., the extent of the stellar disk, is known. The variable inner regions of galaxies, are, however, quite small, and despite either depressions or large excesses of the molecular gas in these regions, they typically only account for a small fraction of the total neutral gas mass ( $\sim 15\%$  on

average in our sample).

We examine this conclusion in Figure 4, which shows the total gas mass of the galaxies in Figure 3 as measured in the respective H I and H<sub>2</sub> intensity maps, compared to the predictions made using Equation 2 (where the integration is carried out to  $2 \times r_{25}$ ). We estimate the uncertainty on the total gas masses derived from the intensity maps (x-axis) from the calibration uncertainties of the THINGS and HERACLES data (5% and 20%, respectively, Walter et al. 2008; Leroy et al. 2009). We thus adopt 20% as the overall uncertainty. For the masses derived from the fit (y-axis), we estimate the uncertainty from error propagation (from Equation 2). We take into account the uncertainties on the fit (slope and

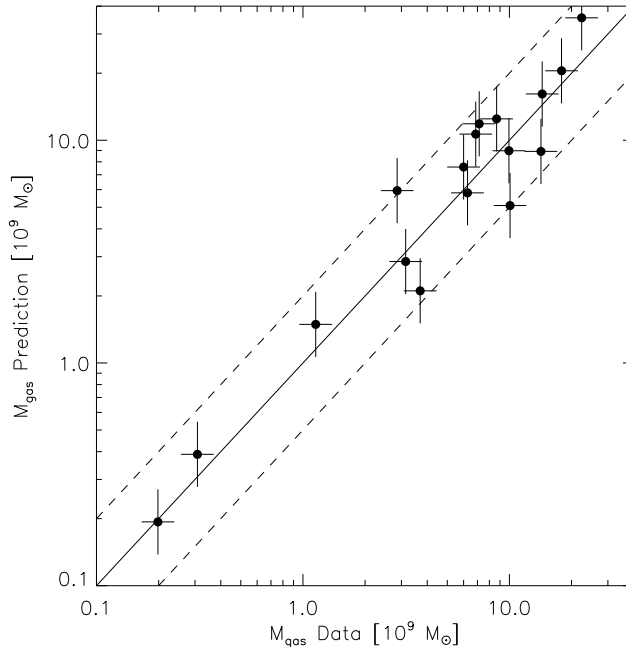


FIG. 4.— Total (H I+H<sub>2</sub>) gas mass obtained from the average radial profile fit (Figure 3 and Equation 2) versus the mass obtained directly from the H I and H<sub>2</sub> intensity maps. The flux is computed out to two optical radii  $r_{25}$  for each of the non-interacting galaxies shown in Figure 3. The solid line indicates unity and the two dashed lines a factor of two scatter. The plot thus shows that Equation 2 allows us to predict the total gas mass of a disk galaxy within a factor of two uncertainty.

intercept),  $r_{25}$  (estimated from Paturel et al. 1991) and  $\Sigma_{\text{trans}}$  (from Leroy et al. 2008). This results in an uncertainty estimate of  $\sim 40\%$  for the mass prediction. Both uncertainties are indicated as error bars in Figure 4.

Figure 4 shows that this equation offers a robust way to predict the total gas mass of disk galaxies to within a factor of two (indicated by the dashed lines, the solid line indicates unity). The mean ratio of predicted versus measured total gas mass is 1.17 (with standard deviation 0.36), which underlines the good correspondence between prediction and data. This close correspondence is rooted in the tightly constrained fit in Figure 3, which falls almost directly on the means in the individual radius bins.

Based on observed metallicity gradients across galaxy disks (e.g., Moustakas et al. 2010), one might speculate about a similarly radially varying CO-to-H<sub>2</sub> conversion factor. Recent work indeed suggests that systematic variations of  $X_{\text{CO}}$  with radius (albeit not necessarily driven primarily by metallicity) occur in at least some of the galaxies studied in this paper: in these cases,  $X_{\text{CO}}$  is observed to increase with increasing radius (Sandstrom et al., in prep.). A low value for  $X_{\text{CO}}$  in galaxy centers seems to be a more common feature (Sandstrom et al., in prep.). The former effect would lead to shallower H<sub>2</sub> profiles, while the latter might in fact explain the observed apparent H<sub>2</sub> excesses in galaxy centers, possibly even giving rise to truly exponential H<sub>2</sub> profiles including the centers.

One of the implications of a universal gas profile is that there appears to be some mechanism that keeps the relationship constant in the face of star formation in these galaxies. For example, Bigiel et al. (2008); Leroy et al. (2008); Bigiel et al. (2011) show that the depletion time

for the molecular gas in disk galaxies is  $\sim 2 \times 10^9$  yr. The region of Figure 3 where  $\frac{\Sigma_{\text{gas}}}{\Sigma_{\text{trans}}} > 1$  (roughly for  $r < 0.45 \times r_{25}$ ) is the region dominated by molecular gas and that gas will therefore be exhausted in about 15% of a Hubble time. In order to keep the profiles self-similar, this implies that either new gas comes from outside the disk and falls preferentially in the central regions, an unlikely occurrence, or that gas flows through the disk to make up the gas lost to star formation, which takes place preferentially within  $r < 0.45 \times r_{25}$ . In either case, it is difficult to understand why the total gas profiles would be so self-similar. For the infall case, one expects such infall to be sporadic, possibly occurring in the form of small galaxies merging with the bigger disk galaxies in our sample. For the inflow case, Figure 3 encompasses a variety of galaxy types and morphologies, and it is hard to see how inflow could be so closely regulated to produce the tight observed relationship.

As cosmological simulations of galaxy evolution including gas become ever more refined, it will become necessary for these simulations to reproduce the universal relationship when carried out to the present epoch. Because of the limitations in making observations of the atomic gas to higher redshift with present day instrumentation, it will be difficult in the near future to extend the work presented here to normal disk galaxies at significantly higher redshifts. It will also be a challenge to extend this work to lower metallicity systems, where CO emission becomes an increasingly poor tracer of the molecular hydrogen (e.g., Bolatto et al. 2011). On the other hand,  $r_{25}$  can be determined in many galaxies to higher redshifts and Equation 2 could be used to estimate  $M_{\text{gas}}$ . As it becomes possible to measure *total* neutral gas masses

to higher redshifts with ALMA, the JVLA, and Arecibo, direct comparisons of the predicted and measured total mass of neutral gas can be extended both to higher redshift and to a larger sample of local galaxies providing good tests of the universality of the neutral gas profile presented in this paper.

The universal gas profile we have described seems to be a fundamental property of normal disk galaxies at  $z = 0$ . We have, however, only probed galaxies of near solar metallicity and none of the galaxies in our final sample are dwarfs. Also, Young et al. (2011) and Serra et al. (2012) have shown recently that a surprisingly large fraction of early type galaxies, i.e., ellipticals and lenticu-

lars, contain large amounts of atomic and molecular gas. Whether these galaxies obey the same universal gas profile is still to be determined.

We thank T. Dame for providing a copy of his Milky Way data compilation and A. Schruba for making available his CO stacking data. This work was supported by Sonderforschungsbereich SFB 881 “The Milky Way System” of the German Research Foundation (DFG) and NSF grant No. 1140031 to the University of California at Berkeley.

## REFERENCES

- Bigiel, F., Leroy, A., Walter, F., Brinks, E., de Blok, W. J. G., Madore, B., & Thornley, M. D. 2008, *AJ*, 136, 2846
- Bigiel, F., Leroy, A. K., Walter, F., et al. 2011, *ApJ*, 730, L13
- Blitz, L., & Rosolowsky, E. 2004, *ApJ*, 612, L29
- Bolatto, A. D., Leroy, A. K., Jameson, K., et al. 2011, *ApJ*, 741, 12
- Cayatte, V., Kotanyi, C., Balkowski, C., & van Gorkom, J. H. 1994, *AJ*, 107, 1003
- Dame, T. M. 1993, “Back to the Galaxy”, AIP Conference Proceedings, 278, 267
- Digel, S. W. 1991, Ph.D. Thesis, Harvard University
- Fich, M., & Blitz, L. 1984, *ApJ*, 279, 125
- Helfer, T. T., Thornley, M. D., Regan, M. W., et al. 2003, *ApJS*, 145, 259
- Kennicutt, R. C., Jr. 1998, *ApJ*, 498, 541
- Kulkarni, S. R., Heiles, C., & Blitz, L. 1982, *ApJ*, 259, L63
- Leroy, A. K., Walter, F., Brinks, E., et al. 2008, *AJ*, 136, 2782
- Leroy, A. K., Walter, F., Bigiel, F., et al. 2009, *AJ*, 137, 4670
- Leroy, A. K., Bigiel, F., de Blok, W. J. G., et al. 2012, *AJ*, 144, 3
- Martin, C. L., & Kennicutt, R. C., Jr. 2001, *ApJ*, 555, 301
- Moustakas, J., Kennicutt, R. C., Jr., Tremonti, C. A., et al. 2010, *ApJS*, 190, 233
- Paturel, G., Garcia, A. M., Fouque, P., & Buta, R. 1991, *A&A*, 243, 319
- Regan, M. W., Thornley, M. D., Helfer, T. T., et al. 2001, *ApJ*, 561, 218
- Schechter, P. L., Aaronson, M., Cook, K. H., & Blanco, V. M. 1988, *The Outer Galaxy*, 306, 31
- Schneider, S. E., & Terzian, Y. 1983, *ApJ*, 274, L61
- Schruba, A., Leroy, A. K., Walter, F., et al. 2011, *AJ*, 142, 37
- Serra, P., Oosterloo, T., Morganti, R., et al. 2012, *MNRAS*, 422, 1835
- Walter, F., Brinks, E., de Blok, W. J. G., et al. 2008, *AJ*, 136, 2563
- Wong, T., & Blitz, L. 2002, *ApJ*, 569, 157
- Young, J. S., & Scoville, N. 1982, *ApJ*, 258, 467
- Young, L. M., Bureau, M., Davis, T. A., et al. 2011, *MNRAS*, 414, 940